



# Peningkatan Performa Aerodinamika NACA 4415 dengan Menggunakan Cavity

## *Aerodynamic Performance Improvement on NACA 4415 Airfoil by Using Cavity*

James Julian<sup>1\*</sup>, Waridho Iskandar<sup>1</sup>, Fitri Wahyuni<sup>1</sup>, dan Nely Toding Bunga<sup>2</sup>

<sup>1</sup>Mechanical Engineering, Universitas Pembangunan Naional Veteran Jakarta, Jawa Barat 12450, Indonesia

<sup>2</sup>Program Studi Teknik Mesin, Fakultas Teknik, Universitas Pancasila, Jakarta 12640, Indonesia

### Article information:

Received:  
24/11/2022  
Revised:  
09/12/2022  
Accepted:  
12/12/2022

### Abstract

*This study uses a numerical method to analyze the cavity's use on the airfoil's trailing edge and the aerodynamic effects it generates. The type of airfoil used is NACA 4415. The variations in the Reynolds number examined in this study are  $2 \times 10^5$  and  $3 \times 10^5$ . The governing equation is the Reynolds Averaged Navier-Stokes paired with the  $k-\epsilon$  turbulence model. This study concludes that the cavity can increase  $C_l$  in the airfoil but cannot delay the stall. The increase in  $C_d$  is also a negative effect of using a cavity in the airfoil. The cavity can increase  $C_l$  by increasing the pressure on the lower side near the trailing edge. Meanwhile, the cavity increases  $C_d$  because it creates a separation of the fluid flow, forming a vortex when viewed in a streamlined form of fluid flow.*

**Keywords:** aerodynamics, cavity, NACA 4415, Reynolds number.

### SDGs:



### Abstrak

Penelitian ini menggunakan metode numerik untuk menganalisis penggunaan cavity di trailing edge airfoil dan efek aerodinamika yang ditimbulkan. Jenis airfoil yang digunakan adalah NACA 4415. Penelitian ini menggunakan variasi bilangan Reynolds  $2 \times 10^5$  dan  $3 \times 10^5$ . Persamaan pengatur yang digunakan adalah Reynolds Averaged Navier-Stokes (RANS) yang dipasangkan dengan model turbulensi  $k-\epsilon$ . Studi ini menghasilkan kesimpulan bahwa cavity memang dapat meningkatkan  $C_l$  pada *airfoil*, akan tetapi tidak mampu menunda stall. Peningkatan  $C_d$  juga menjadi efek negative dari penggunaan cavity di airfoil. Cavity dapat meningkatkan  $C_l$  dengan cara memperbesar tekanan di lower side dekat trailing edge. Sementara itu cavity meningkatkan  $C_d$  karena menimbulkan adanya separasi aliran fluida yang membentuk suatu pusaran jika dilihat dalam bentuk *streamline* aliran fluida.

**Kata Kunci:** aerodinamika, cavity, NACA 4415, bilangan Reynolds.

\*Correspondence Author. Phone: -; Handphone: +62 878 8343 9097  
email : [zames@upnvj.ac.id](mailto:zames@upnvj.ac.id)



This work is licensed under a [Creative Commons Attribution-NonCommercial 4.0 International License](https://creativecommons.org/licenses/by-nc/4.0/)

## 1. INTRODUCTION

Analysis of airfoil aerodynamic performance has been a topic of interest in the last few decades (Megawanto *et al.*, 2018). By increasing the aerodynamic capabilities of the airfoil, its utilization will be more widespread and efficient (Megawanto *et al.*, 2019). Increasing the aerodynamic capabilities of the airfoil can be done by increasing the lift force that can be generated by the airfoil, known as high-lift devices. However, to produce airfoils into high-lift devices, several challenges and problems must be faced (Harinaldi *et al.*, 2016, 2020). One of the biggest challenges is that the fluid flow around the airfoil at low Reynolds numbers is very complex. In addition, airfoils also experience various phenomena, such as adverse pressure gradients, flow separation, and confluent boundary layers (Julian, Iskandar, Wahyuni, Ferdianto, *et al.*, 2022). Unfortunately, the fluid flow velocity is generally at a low Reynolds number if the airfoil is used as a wind turbine (Kosasih, Karim and Julian, 2019). Thus, the utilization of the airfoil as a wind turbine is not optimal. Another improvement in the aerodynamic capabilities is to minimize the drag force generated due to the interaction of the airfoil with the fluid flow (Julian *et al.*, 2016; Julian, Harinaldi and Budiarto, 2016; Harinaldi *et al.*, 2019). Drag force can cause negative effects on various devices; on vehicles, drag force can result in the wastage of fuel (Julian *et al.*, 2018; Kosasih, Karim and Julian, 2019). It also needs to get more attention because the cross-sectional shape of the airplane wing adopts the airfoil shape. Overall, further study is needed to optimize the aerodynamic capabilities of an airfoil.

Several studies to improve airfoil capability have been carried out. Liu *et al.*, studied to improve the aerodynamic capabilities of NACA 4415 by using grooves (Liu *et al.*, 2020). Grooves are installed at 16% of the chord length. There are two types of groove variations: rectangular grooves and arc grooves. The rectangular grooves show a better performance improvement than the arc grooves. The groove can improve airfoil

performance by increasing coefficient lift ( $C_l$ ) at  $1^\circ \leq \text{Angle of Attack (AoA)} \leq 11^\circ$ . Meanwhile, coefficient drag ( $C_d$ ) in the airfoil at the same interval, namely  $1^\circ \leq \text{AoA} \leq 11^\circ$  (Liu *et al.*, 2020). Yousefi *et al.* conducted a computational study on NACA 0012 airfoils that were given suction and blowing. The maximum increase in airfoil performance is obtained at the suction location of 2.5% of the chord length (Yousefi, Saleh and Zahedi, 2014). Julian *et al.*, studied to improve the performance of NACA 0015 using the co-flow jet technique method. This method combines suction and blowing into a unified whole. The research was carried out computationally using a structured mesh type. Co-flow jet proved effective for increasing  $C_l$  with a percentage of 114%. In addition, co-flow jets can also reduce  $C_d$  by a percentage of 24% (Julian, Iskandar, Wahyuni, Armansyah, *et al.*, 2022). Aziz and Islam investigated the effect of the cavity on the lower side of NACA 4415 computationally and experimentally. The results obtained from these studies are cavity can increase  $C_l$  by 15.75%. However, the cavity also increases  $C_d$  by 10.57% (Aziz and Islam, 2017).

Based on all the research mentioned in the paragraph above, it can be concluded that there are various ways to improve the performance of the airfoil. The best way is to use active flow control methods such as suction, blowing, and co-flow jet technique (Julian *et al.*, 2017; Harinaldi *et al.*, 2019). However, this type of device is less effective because it requires additional energy to perform suction or blow a fluid stream (Harinaldi *et al.*, 2019). Groove is a passive flow control device that is only effective at moderate AoA. When AoA is close to an extreme, this method must be more effective and reduce  $C_l$ . The most effective way is to use a cavity. Therefore, this study aims to analyze and reveal the effect of using a cavity on the airfoil. It will provide a more thorough and specific understanding. The fluid flow pattern in the cavity area is also an interesting research object. By examining this more deeply, the causes of the increase in aerodynamic performance or things that still need to be improved from the existing cavity shape will be identified.

## 2. METHODOLOGY

### 2.1. Step Cavity on The Airfoil

This research modifies the airfoil's shape into a backward-facing step shape to improve its performance of the airfoil. Thus, an airfoil design that resembles Kline-Fogleman airfoils will be produced (Donelli, Gregorio and Iannelli, 2012). Changing the shape of an airfoil will change the entire fluid flow structure through the airfoil. Through this modification, a vortex of trapped fluid flow will be generated (Vuddagiri and Samad, 2013). In this study, the dimensions of the airfoil and the step cavity can be seen in Figure 1.

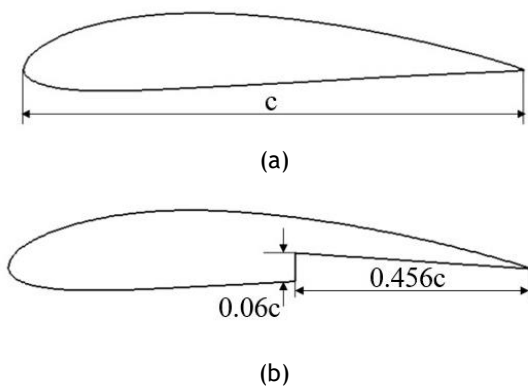


Figure 1. Tested airfoil (a) NACA without cavity (b) NACA 4415 with cavity

### 2.2. Step Cavity on The Airfoil

The backward-facing step is a fluid flow model that is quite common. In this study, the backward-facing step occurs in the cavity area (Scharnowski, Bolgar and Kähler, 2016). The geometry to form this fluid flow model is quite simple, but the fluid flow generated from this flow model is very complex. In a backward-facing step, fluid flow separation occurs at the corner-facing step (Biswas, Breuer and Durst, 2004). In the separation area, a boundary separates the recirculation area from the free area. This layer will continue to grow as the downstream distance increases until it reaches the reattachment area. Overall the backward-facing step is shown in Figure 2 (Scharnowski, Bolgar and Kähler, 2016).

### 2.3. Flow Domain and Computation Setup

The flow domain for fluid flow surrounding the airfoil can be seen in Figure 3a (Julian,

Iskandar, Wahyuni and Ferdianto, 2022). All dimensions used are arranged in such a way as to reduce the effect of boundary conditions on the resulting fluid flow. The position of trailing edge is in the center of semi-circle. Further, the computation process uses the negative form of the airfoil to the domain. The domain is governed by velocity inlet boundary conditions and pressure outlet (Julian, Iskandar, Wahyuni, Ferdianto, et al., 2022).

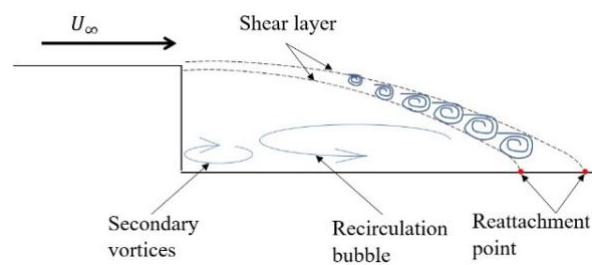
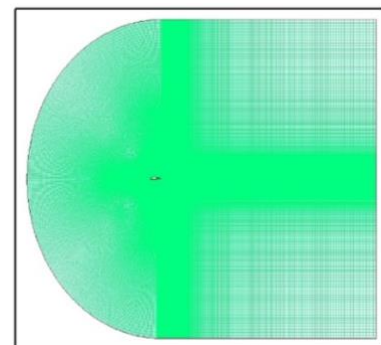
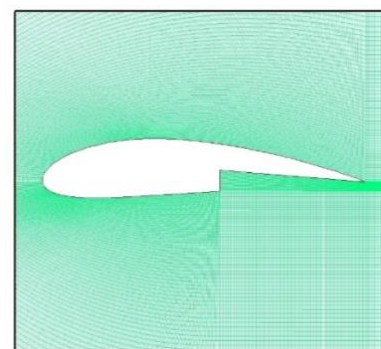


Figure 2. Test loading standard



(a)



(b)

Figure 3. Mesh configurations (a) domain (b) around the airfoil

On the other hand, an airfoil is defined as a wall (no slip). The computational process uses the RANS equation combined with the standard  $k-\epsilon$  turbulence model.

The mathematical equation for RANS can be seen in equations 1 and 2. Meanwhile, the mathematical form of the k-ε turbulence model can be seen in equations 3 and 4 (Iskandar *et al.*, 2022).

$$\frac{\partial \rho}{\partial t} + \frac{\partial}{\partial x_i} (\rho u_i) = 0 \quad (1)$$

$$\begin{aligned} \frac{\partial}{\partial t} (\rho u_i) + \frac{\partial}{\partial x_j} (\rho u_i u_j) &= \frac{\partial p}{\partial x_i} + \frac{\partial}{\partial x_j} \\ \left[ \mu \left( \frac{\partial u_i}{\partial x_j} + \frac{\partial u_j}{\partial x_i} - \frac{2}{3} \delta_{ij} \frac{\partial u_k}{\partial x_k} \right) \right] & \quad (2) \\ + \frac{\partial}{\partial x_j} (-\overline{\rho u_i u_j}) & \end{aligned}$$

$$\begin{aligned} \frac{D}{Dt} (\rho k) &= \frac{\partial}{\partial x_j} \left[ \left( \mu + \frac{\mu_t}{\sigma_k} \right) \frac{\partial k}{\partial x_j} \right] & (3) \\ + G_k - \rho \varepsilon & \end{aligned}$$

$$\begin{aligned} \frac{D}{Dt} (\rho \varepsilon) &= \frac{\partial}{\partial x_j} \left[ \left( \mu + \frac{\mu_t}{\sigma_\varepsilon} \right) \frac{\partial \varepsilon}{\partial x_j} \right] + & (4) \\ C_{\varepsilon 1} \frac{\varepsilon}{k} G_k - \rho C_{\varepsilon 2} \frac{\varepsilon^2}{k} & \end{aligned}$$

## 2.4. Mesh and Mesh Independence Test

This study uses a structured quadrilateral mesh, as shown in Figure 3. The number of elements offered is 50,000, 100000, and also 200000. Three types of mesh are then analyzed with a mesh independence test to determine which is most suitable for other computational processes. The mesh with smallest error will be selected. In this study, the mesh independence test for this study uses Richardson extrapolation, which is generalized by Roache (Iskandar *et al.*, 2022). All data used in this activity can be seen in Table 1. The data is taken at coordinates X=0.5 and Y=0.15. This study uses the reference point right on the airfoil's leading edge. The results of the mesh independence test show that  $\frac{GCI_{coarse}}{GCI_{fine}} r^p \approx 1$  so that it can be concluded that the variation in the number of meshes is in the convergence index

range . The value closest to the parameter is the fine mesh, as shown in Figure 4, in other words, the fine mesh gives the lowest error value of 0.126%. Meanwhile, the medium mesh has an error value of 0.402%, and the coarse mesh has an error value of 1.287%. Thus, further computational processes will use a fine mesh with a total of 200,000 elements.

Table 1. Mesh independence test data

Number of elements	Mesh classification	Velocity sample	symbol
2×10 <sup>6</sup>	Fine	1.806	f <sub>1</sub>
10 <sup>6</sup>	Medium	1.801	f <sub>2</sub>
5×10 <sup>5</sup>	Coarse	1.798	f <sub>3</sub>

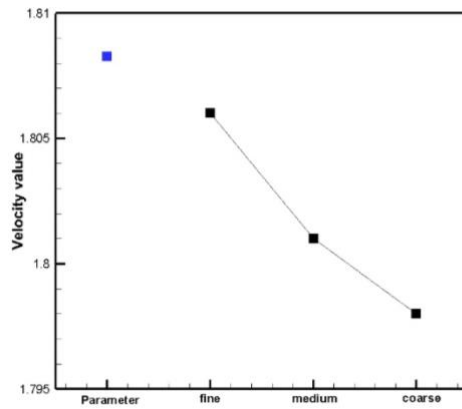
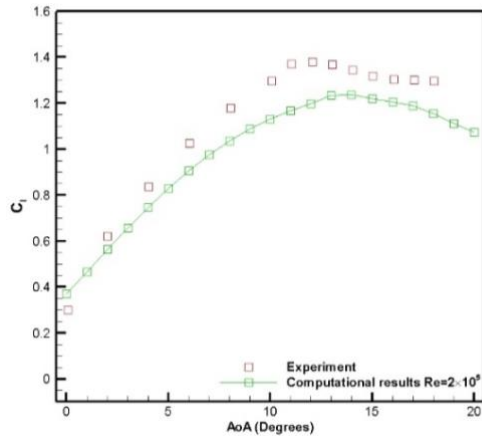


Figure 4. Mesh independence test

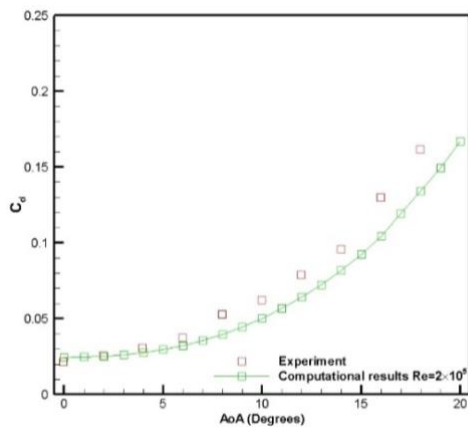
## 3. RESULTS AND DISCUSSION

The analysis in this study was carried out on the Reynolds numbers 2×10<sup>5</sup> and 3×10<sup>5</sup>. However, before that, validation is carried out first to ensure that all computational processes have been carried out correctly. Validation was carried out on the Reynolds number 2×10<sup>5</sup>. Data that used as a validation is from Sudhakar *et al.* (Senthamarai, Venkatakrishnan and N, 2020). The validation results can be seen in Figure 5. Figure 5a is a curve of the coefficient of lift (C<sub>l</sub>). Meanwhile, Figure 5b is a curve of the coefficient of drag (C<sub>d</sub>). The computational and experimental results show similarities in terms of the trend of the curves. Even though there is a slight difference when the AoA is large enough, this is

still acceptable because, at this AoA, the fluid flow becomes more complex. A vortex around the upper side of the airfoil causes this complexity. The complexity of the vortex is complicated to be predicted by numerical methods (Bao et al., 2020).



(a)

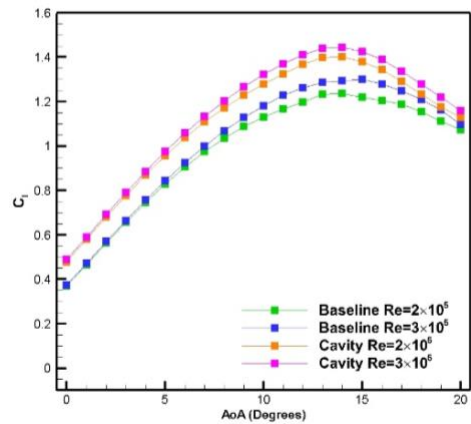


(b)

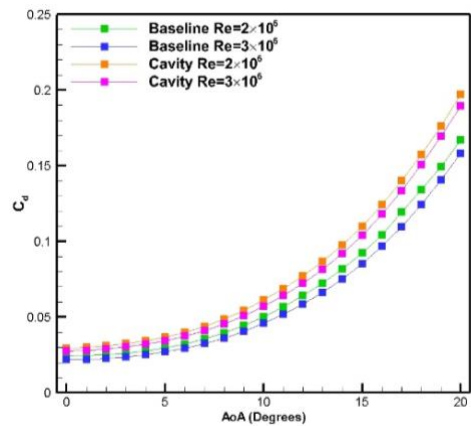
Figure 5. Aerodynamics validation by (a)  $C_l$  (b)  $C_d$

Figure 6a shows  $C_l$  at the Reynolds number  $2 \times 10^5$  and  $3 \times 10^5$  for the baseline airfoil and cavity. The cavity can significantly increase the  $C_l$  in the airfoil in all AoA. If the Reynolds number of the airfoil is  $2 \times 10^5$ , the use of a cavity does not change the AoA stall of the airfoil. Where the stall still occurs at  $AoA=15^\circ$ . Meanwhile, a cavity accelerates the airfoil stall for the Reynolds number  $3 \times 10^5$ . The baseline produces a stall at  $AoA=16^\circ$  while the airfoil modified with a cavity produces a stall at  $AoA=15^\circ$ . Besides that, the cavity on the trailing edge also has a negative impact, increasing the airfoil's  $C_d$ . This increase in

$C_d$  can be observed in all variations of the Reynolds number and AoA. It can be observed in Figure 6b. A vortex causes an increase in  $C_d$  in the cavity area. Furthermore, this problem is deepened in the following discussion.



(a)



(b)

Figure 6. Aerodynamics baseline and cavity validation by (a)  $C_l$  (b)  $C_d$

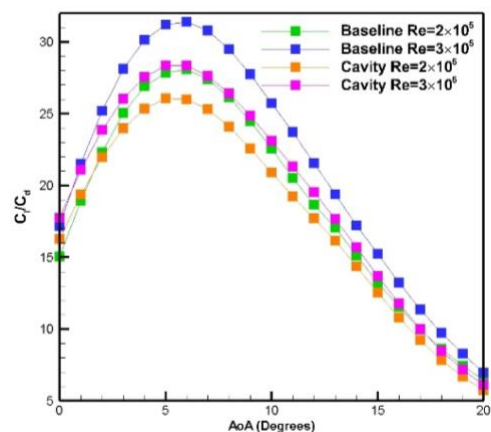
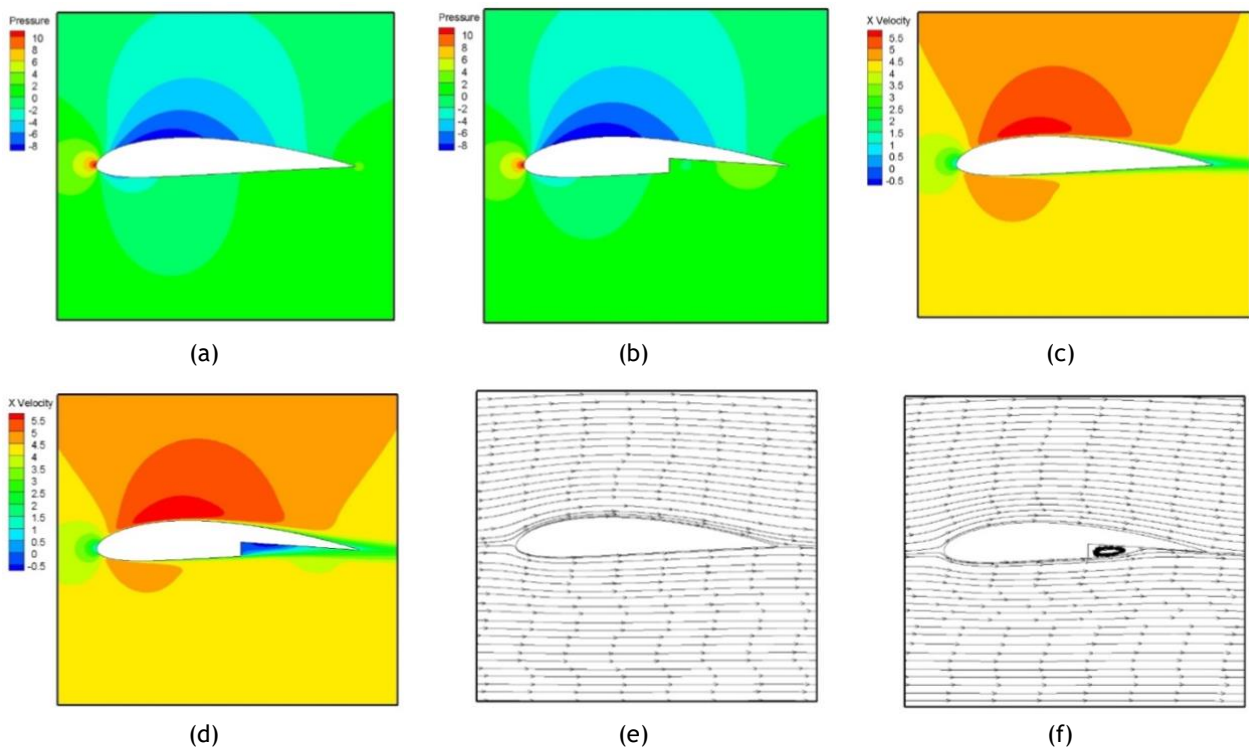


Figure 7. Aerodynamic performance

The aerodynamic performance of a streamlined object such as an airfoil can be seen from two aspects, namely  $C_l$  and  $C_d$ . Thus, it can be seen at what angle of attack the airfoil shows the most efficient performance. The most efficient performance is at the peak of the  $C_l/C_d$  curve. Figure 7 shows the  $C_l/C_d$  curves at various variations of AoA. In general, the cavity reduces the aerodynamic performance of the airfoil. It means the resulting increase in  $C_d$  becomes more dominant compared to the increase in  $C_l$ . It applies to the Reynolds number  $2 \times 10^5$  and the Reynolds number  $3 \times 10^5$ . Even at the Reynolds number  $3 \times 10^5$ , there is no change in the most effective AoA in the airfoil, namely at AoA =  $6^\circ$ . Meanwhile, at the Reynolds number of  $2 \times 10^5$ , the most effective reduction in AoA from the airfoil occurs, where at the baseline, the most effective AoA from the airfoil is AoA= $6^\circ$ , while in an airfoil with a cavity, the most effective AoA is AoA= $5^\circ$ .

The following discussion is about fluid flow visualization around the airfoil. An analysis is carried out using various fluid flow contours. The analysis was carried out at AoA= $0^\circ$  with a Reynolds number of  $3 \times 10^5$ . Through this analysis, the causes of various changes in the aerodynamic performance of the airfoil can be identified. Figure 8b shows that using a cavity increases the pressure near the airfoil's trailing edge. It is what causes an increase in  $C_l$ . Meanwhile, Figure 8c and Figure 8d explain the velocity contour on the baseline airfoil and airfoil with cavity respectively. The cavity causes fluid flow with negative velocity. This negative velocity is the separation of the fluid flow in the cavity. If this flow is seen in a streamlined fluid flow i.e., Figure 8e and Figure 8f, a vortex will be seen in the cavity. This vortex is the main cause of the increase in  $C_d$  in the airfoil.



**Figure 8.** Flow visualization (a) pressure contour baseline airfoil (b) pressure contour cavity airfoil (c) velocity contour baseline airfoil (d) velocity contour cavity airfoil (e) streamline baseline airfoil (f) streamline airfoil with cavity

#### 4. CONCLUSIONS

This study produced several conclusions that can be used as an overall summary. Using a cavity on the airfoil's trailing edge can increase  $C_l$  at the Reynolds number of  $2 \times 10^5$  and  $3 \times 10^5$ . However, the cavity cannot delay the stall on the airfoil. At the Reynolds number  $2 \times 10^5$ , the stall is still at  $AoA=15^\circ$ . Meanwhile, when the Reynolds number was changed to  $3 \times 10^5$ , the stall accelerated by  $1^\circ$  from the previous  $AoA=16^\circ$  to  $AoA=15^\circ$ . The cavity can also increase the  $C_d$  of the airfoil in all variations of Reynolds and AoA groups. A change in pressure near the airfoil's trailing edge causes an increase in  $C_l$  in the airfoil. Meanwhile, the increase in  $C_d$  was caused by fluid flow separation in the cavity location. This fluid flow separation looks like a vortex when viewed in a streamlined form of fluid flow.

#### REFERENCES

- Aziz, Md.A.B. and Islam, Md.S. (2017) 'Effect of Lower Surface Modification on Aerodynamic Characteristics of an Airfoil', in *Proceedings of the International Conference on Mechanical Engineering and Renewable Energy 2017 (ICMERE2017)*. International Conference on Mechanical Engineering and Renewable Energy 2017 (ICMERE2017), Bangladesh: ICMERE, pp. 1-6.
- Bao, H. et al. (2020) 'Numerical simulation of flapping airfoil with alula', *International Journal of Micro Air Vehicles*, 12, pp. 1-15.
- Biswas, G. et al. (2004) 'Backward-Facing Step Flows for Various Expansion Ratios at Low and Moderate Reynolds Numbers', *Journal of Fluids Engineering*, 126(3), pp. 362-374.
- Donelli, R., Gregorio, F.D. and Iannelli, P. (2012) 'Flow Separation Control by Trapped Vortex', in *48th AIAA Aerospace Sciences Meeting Including the New Horizons Forum and Aerospace Exposition*. Florida: American Institute of Aeronautics and Astronautics (AIAA 2010-1409), pp. 1-12.
- Harinaldi et al. (2016) 'The effect of plasma actuator on the depreciation of the aerodynamic drag on box model', *AIP Conference Proceedings*, 1737(1), p. 040004.1-040004.5.
- Harinaldi et al. (2019) 'The comparison of an analytical, experimental, and simulation approach for the average induced velocity of a dielectric barrier discharge (DBD)', in *AIP Conference Proceedings. The 10th International Meeting of Advances in Thermofluids (IMAT 2018)*, AIP Publishing LLC, p. 020027.1-020027.8.
- Harinaldi et al. (2020) 'Flow Control with Multi-DBD Plasma Actuator on a Delta Wing', *Evergreen*, 7(4), pp. 602-608.
- Iskandar, W. et al. (2022) 'Study of Airfoil Characteristics on NACA 4415 with Reynolds Number Variations', *International Review on Modelling and Simulations (IREMOS)*, 15(3), pp. 162-171.
- Julian, J. et al. (2016) 'The Effect of Plasma Actuator Placement on Drag Coefficient Reduction of Ahmed Body as an Aerodynamic Model', *International Journal of Technology*, 7(2), pp. 306-313.
- Julian, J. et al. (2017) 'Review: Flow Control on a Squareback Model', *International Review of Aerospace Engineering (IREASE)*, 10(4), pp. 230-239.
- Julian, J. et al. (2018) 'Effect of plasma actuator in boundary layer on flat plate model with turbulent promoter', *Proceedings of the Institution of Mechanical Engineers, Part G: Journal of Aerospace Engineering*, 232(16), pp. 3001-3010.
- Julian, J., Iskandar, W., Wahyuni, F., Ferdianto, et al. (2022) 'Characterization of the Co-Flow Jet Effect as One of the Flow Control Devices', *Jurnal Asimetrik: Jurnal Ilmiah Rekayasa & Inovasi*, 4(2), pp. 185-192.
- Julian, J., Iskandar, W., Wahyuni, F. and Ferdianto, F. (2022) 'Computational Fluid Dynamics Analysis Based on The Fluid Flow Separation Point on The Upper Side of The NACA 0015 Airfoil With The Coefficient of Friction', *Media Mesin: Majalah Teknik Mesin*, 23(2), pp. 70-82.
- Julian, J., Iskandar, W., Wahyuni, F., Armansyah, A., et al. (2022) 'Effect of Single Slat and Double Slat on Aerodynamic Performance of NACA 4415', *International Journal of Marine Engineering Innovation and Research*, 7(2), pp. 93-100.

- Julian, J., Harinaldi and Budiarmo (2016) 'The effect of plasma actuator utilization to the reduction of aerodynamic drag of cylinder and box models', in *Proceedings of 12th International Conference on Heat Transfer, Fluid Mechanics and Thermodynamics. 12th International Conference on Heat Transfer, Fluid Mechanics and Thermodynamics*, Spain: University of Pretoria, pp. 833-838.
- Kosasih, E.A., Karim, R.F. and Julian, J. (2019) 'Drag reduction by combination of flow control using inlet disturbance body and plasma actuator on cylinder model', *Journal of Mechanical Engineering and Sciences*, 13(1), pp. 4503-4511.
- Liu, Y. *et al.* (2020) 'Numerical study of the effect of surface grooves on the aerodynamic performance of a NACA 4415 airfoil for small wind turbines', *Journal of Wind Engineering and Industrial Aerodynamics*, 206, p. 104263.1-104263.12.
- Megawanto, F.C. *et al.* (2018) 'Numerical analysis of plasma actuator for drag reduction and lift enhancement on NACA 4415 airfoil', *AIP Conference Proceedings*, 2001, p. 050001.1-050001.6.
- Megawanto, F.C. *et al.* (2019) 'Flow separation delay on NACA 4415 airfoil using plasma actuator effect', *International Review of Aerospace Engineering*, 12(4), pp. 180-186.
- Scharnowski, S., Bolgar, I. and Kähler, C.J. (2016) 'Characterization of Turbulent Structures in a Transonic Backward-Facing Step Flow', *Flow, Turbulence and Combustion*, 98, pp. 947-967.
- Senthamarai, S., Venkatakrisnan, L. and N, R. (2020) 'The influence of leading-edge tubercles on airfoil performance at low Reynolds numbers', in *Proceedings of AIAA SciTech Forum. AIAA SciTech Forum*, Orlando: AIAA, pp. 1-25.
- Vuddagiri, A. and Samad, A. (2013) 'Vortex Trapping by Different Cavities on an Airfoil', *Wind Engineering*, 37(5), pp. 469-482.
- Yousefi, K., Saleh, R. and Zahedi, P. (2014) 'Numerical study of blowing and suction slot geometry optimization on NACA 0012 airfoil', *Journal of Mechanical Science and Technology*, 28(4), pp. 1297-1310.